Available online at www.sciencedirect.com
SCIENCE DIRECT
Journal of Catalysis 232 (2005) 43–50
JOURNAL OF CATALYSIS
www.elsevier.com/locate/jcat

Enantioselective hydrogenation over immobilized rhodium diphosphine complexes on aluminated SBA-15

Adrian Crosman, Wolfgang F. Hoelderich *

Department of Chemical Technology and Heterogeneous Catalysis, RWTH Aachen University, Worringerweg 1, 52074 Aachen, Germany

Received 8 July 2004; revised 26 November 2004; accepted 29 November 2004

Available online 7 April 2005

Abstract

A series of heterogeneous chiral catalysts was prepared from rhodium diphosphine complexes [Rh(L-L)COD]Cl ((L-L) = diphosphine ligand and COD = cyclooctadiene) and aluminated SBA-15. Impregnation of mesoporous Al-SBA-15 with organometallic complexes led to strongly bonded hydrogenation catalysts. The complexes were bound to the carrier by the interaction of the cationic rhodium of the organometallic complex with the anionic host framework, and between Al Lewis acid sites and P Lewis basic sites. The hydrogenation of dimethyl itaconate and that of methyl α-acetamidoacrylate were studied as test reactions. The immobilized catalysts showed high activities and excellent chemo- and enantioselectivities. Up to 93% e.e., > 99% conversion, and 99% selectivity were observed in the case of studied prochiral olefins. The catalysts could be reused without loss of catalytic activity. These new catalysts were stable toward leaching of the homogeneous complex from the solid framework.

Keywords: Immobilization; Rhodium; Diphosphine; Alumination; SBA-15; Asymmetric; Hydrogenation

1. Introduction

For economic, environmental, and social reasons, the trend toward the application of optically active compounds is undoubtedly increasing. Among the various methods for selective production of single enantiomers, asymmetric catalysis is the most attractive method from the atom economic point of view [1,2]. Among the numerous types of asymmetric catalysis, the most impressive systems are those for the hydrogenation of carbon–carbon, carbon–nitrogen, and carbon–oxygen bonds with transition metal diphosphine complexes. Asymmetric hydrogenations are of particular industrial relevance because of the high efficiencies that can be obtained with a relatively small environmental impact [3].

Homogeneous catalysts are known to exhibit high selectivity and activity in a variety of asymmetric transformations under relatively mild conditions. In 2001, the significant achievements in the design and application of asymmetric homogeneous catalysts were recognized when the Nobel Prize in chemistry was awarded to W.S. Knowles and R. Noyori for enantioselective hydrogenation catalysis and K.B. Sharpless for enantioselective oxidation catalysis [4–6]. However, despite the huge amount of work devoted to this subject in both academic and industrial fields, the contribution of asymmetric catalysis to the overall production of chiral chemicals is much lower than originally expected [7]. Because of the cost of sophisticated chiral ligands, often exceeding that of the noble metal employed, catalyst recovery is of paramount importance for the application of enantioselective metal catalysis to large-scale processes, eventually in continuous-flow reactors. Furthermore, even if the activity and selectivity of homogeneous catalysts are exceptionally high, toxicological and environmental problems should also be taken into account.

To make the recovery and recycling of asymmetric catalysts easier, successful approaches involve the immobilization of molecular precursors on a support material or in an appropriate phase system so that the catalyst can be quantita-

* Corresponding author. Fax: +49 241 8022291.
E-mail address: hoelderich@rwth-aachen.de (W.F. Hoelderich).

0021-9517/$ – see front matter
doi:10.1016/j.jcat.2004.11.033

tively separated from both product(s) and unreacted reagents by filtration or phase separation. Various routes for the immobilization of organometallic complexes have been investigated, such as covalent bonding of the ligand with the carrier [8–10], entrapment or occlusion in polymer matrices [11,12], immobilization by steric hindrance ("ship-in-the-bottle" concept) [13–15], and adsorption via ionic interactions with the support [16–18]. The topic of immobilization has been the subject of several hundred publications and some reviews [19,20], and the recent one by McMorn and Hutchings [21] has focused on different methodologies used to create immobilized heterogeneous asymmetric catalysts. The main monograph in this field was published in 2000 by Jacobs et al. [22].

Mesoporous molecular sieves have received much attention in the field of catalysis, especially for their use as supports. Ion exchange, catalytic, and adsorptive proprieties of molecular sieve materials originate from acid sites that arise from the presence of accessible hydroxyl groups associated with tetrahedral framework aluminum in a silica framework. A recently discovered pure silica phase, designated SBA-15, has long-range order, large monodispersed mesopores (up to 50 nm), and thicker walls (typically between 3 and 9 nm), which make it more thermally and hydrothermally stable than the M41S-type materials [23–25]. Unfortunately, as the pure silica SBA-15 is synthesized in strong acid media (2 M HCl solution), incorporation of framework aluminum into SBA-15 by direct synthesis seems impossible, because most aluminum sources dissolve in strong acids. Previous studies have shown that aluminum can be effectively incorporated into siliceous SBA-15 via various postsynthesis procedures that include aluminum grafting onto SBA-15 wall surfaces with anhydrous $AlCl_3$ or aluminum isopropoxide in non-aqueous solutions, or sodium aluminate in aqueous solutions followed by calcinations [26,27].

Our research was focused on the use of SBA-15-type materials as the carrier, which are characterized by a well-defined pore structure and high surface area, offering new opportunities for the immobilization of large catalytic species. Here we present a very straightforward method for immobilizing rhodium diphosphine complexes on aluminated SBA-15. This heterogenization is based on ionic interaction between the negatively charged Al-SBA-15 framework and the cationic rhodium of the organometallic complex. This method allowed us to successfully heterogenize homogeneous catalysts without modifying their chemical structure. Furthermore, the activity of the new chiral heterogeneous rhodium diphosphine catalysts in the enantioselective hydrogenation of different prochiral olefins was investigated.

2. Experimental

It is well known that Rh complexes containing diphosphines are very sensitive to water and oxygen. Phosphines can easily be oxidized under such conditions and then lose their catalytic activity. Considering these facts, we carried out all of the experiments involving diphosphines, rhodium diphosphine complexes, and immobilized complexes under dry argon with Schlenk techniques. Moreover, before the immobilization of organometallic complexes on the solid support, the aluminated SBA-15 was calcined overnight at 300 °C in order to remove all adsorbed water molecules.

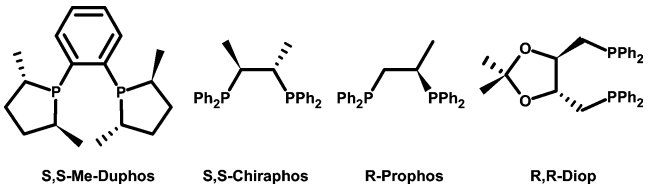

Fig. 1. Used diphosphine ligands.

2.1. Preparation and alumination of SBA-15

Twenty grams of amphiphilic triblock copolymer, poly(ethylene glycol)-block-poly(propylene glycol)-block-poly(ethylene glycol) (average molecular weight 5800; Aldrich), was dispersed in 150 g of water and 600 g of 2 M HCl solution with stirring, followed by the addition of 42 g of tetraethyl orthosilicate to the homogeneous solution with stirring. This gel mixture was stirred continuously at 40 °C for 6 h and finally crystallized in a Teflon-lined autoclave at 90 °C for 3 days. After crystallization the solid product was centrifuged, filtered, washed with deionized water, and dried at 120 °C in air. The material was calcined in static air at 550 °C for 24 h to decompose the triblock copolymer and obtain a white powder (SBA-15) [23]. This white powder was used as the parent material to produce an aluminum-containing material denoted Al-SBA-15.

Silica SBA-15 (10 g, 166.5 mmol Si) was dispersed in 250 mL of dry hexane containing 0.85 g (4.1 mmol Al) aluminum isopropoxide. The resulting suspension was stirred at room temperature for 24 h, and afterward the powder was filtered, washed with dry hexane, and dried at 120 °C in air. This solid Al-SBA-15 was then calcined in static air at 550 °C for 6 h (heating rate 1 °C/min) [25].

2.2. Preparation and immobilization of rhodium diphosphine complexes

All solvents were purified, degassed, and saturated with argon, and the preparation of the Rh complexes was carried out carefully under argon with standard Schlenk techniques. In a Schlenk tube under Ar, 0.075 mmol $[CODRhCl]_2$ was dissolved in 10 mL CH_2Cl_2 and 0.165 mmol diphosphine (S,S-Me-Duphos, S,S-Diop, S,S-Chiraphos and R-Prophos; Fig. 1) was added. The resulting mixture was stirred at RT for 3 h, and then the solvent was eliminated under reduced pressure. The powder obtained was vacuum-dried overnight.

In the case of each diphosphine ligand, an organometallic complex was prepared with the previous method. To immobilize Rh-diphosphine complexes, 1 g Al-SBSA-15 was

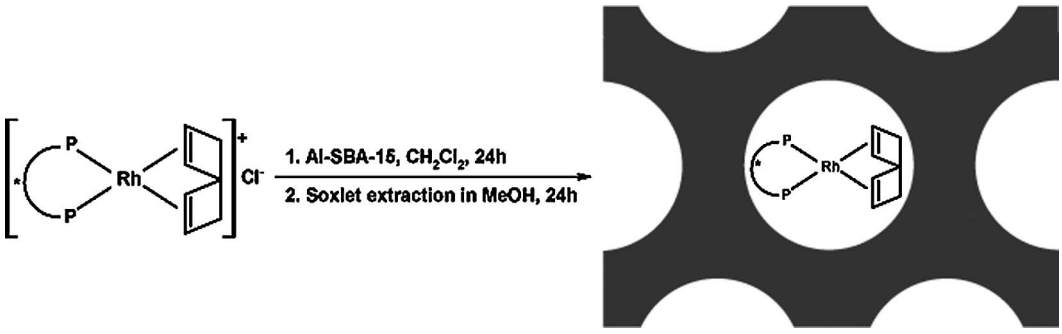

Fig. 2. Immobilization of rhodium diphosphine complexes on Al-SBA-15.

suspended in 9 mL CH_2Cl_2 and stirred at RT for 1 h. The Rh-diphosphine complex (0.15 mmol) was dissolved in 1 mL CH_2Cl_2 and added to the Al-SBA-15/CH_2Cl_2 suspension. The reaction mixture was stirred at RT for 24 h, followed by solvent evaporation under reduced pressure. The recovered solid was Soxhlet washed with MeOH for 24 h to remove any residual free Rh complex. The absence of the homogeneous complex in the mixture was checked by ICP-AES analysis and FT-IR spectroscopy. The final material was vacuum-dried at RT overnight. The heterogeneous catalyst has a pale yellow color similar to the color of the homogeneous complex. Fig. 2 is a simple sketch of the immobilized rhodium diphosphine complexes on Al-SBA-15.

2.3. Catalytic tests

Hydrogenation of dimethylitaconate and methyl α-acetamidoacrylate was carried out in glass autoclaves at ambient temperature and 3 bar of hydrogen pressure for 24 h. The catalyst was added to a solution of 2 mmol of olefin in 10 mL of methanol. The heterogeneous catalysts were recycled with standard methods (the catalyst was filtered off, washed with 5 mL MeOH, dried overnight at room temperature, and reused in the next cycle at the same substrate/catalyst ratio).

2.4. Characterization

X-Ray powder diffraction patterns were collected on a Siemens Diffractometer D5000 equipped with a secondary monochromator, a variable diaphragm V 20, and a nickel filter, with the use of Cu-K_α radiation (wavelength 1.5406 Å); the angle speed was $0.02\,^\circ/\text{min}^{-1}$. Bulk elemental chemical analyses were done with inductive couple plasma atomic emission spectroscopy (ICP-AES) on a Spectroflame D (Spectro Analytic Instrument). Nitrogen adsorption/desorption isotherms at liquid nitrogen temperature were measured on a Micromeritics ASAP 2010 instrument. The samples were pre-outgassed at 150 °C. The pore diameter and specific pore volume were calculated according to the Barrett–Joyner–Halenda (BJH) theory. The specific surface area was obtained with the Brunauer–Emmett–Teller (BET) equation.

FT-IR analyses were done on a Nicolet Protégé 460, equipped with an evacuable furnace cell with KBr windows, containing the sample wafer. Without the use of a binder, the samples were pressed into a self-supporting wafer and, after being mounted on the sample cell, were dried at 200 °C and 10^{-3} mbar for 16 h. Adsorbed pyridine spectra were taken with a Nicolet Protégé 460 equipped with an evacuable furnace cell with a KBr windows, containing the sample wafer. The samples were pressed into a self-supported wafer and, after being mounted on the sample cell, were dried at 200 °C and 10^{-3} mbar for 16 h. After the cell was cooled to 50 °C the background spectra were recorded. Spectra were always collected as an average of 200 runs with 0.5 cm^{-1} definition. The pyridine adsorption was carried out as follows: the catalyst was equilibrated three times with pyridine vapors at 50 °C, the cell was shut off from vacuum, and flask containing pyridine was opened to the cell. After 60 min of evacuation a spectrum was recorded. The desorption of the probe molecule was successively monitored stepwise, by evacuation of the sample for 60 min at 50, 100, and 200 °C and cooling to 50 °C between each step, to record the spectrum.

For thermogravimetric analysis a Netzsch 209/2/E equipped with a STA409 controller was used. The heating rate was 5 °C/min, and α-Al_2O_3 was used as a reference material. Temperature-programmed desorption of ammonia was measured on a TPDRO 1100 apparatus from CE Instruments. First, the materials were calcined for 2 h at 500 °C under argon, followed by ammonia loading at 100 °C (3% NH_3 in argon, 2 h). Subsequently, the system was purged with argon for 2 h, then NH_3 was desorbed by heating with 25 °C/min to 900 °C under flowing argon.

The solid-state NMR spectra were recorded on a Bruker DSX 500 spectrometer equipped with a 2.5-mm CP/MAS probe head. In the case of the ^{31}P-MAS NMR spectra, 5000–10000 transients gave satisfactory signal-to-noise ratios. The samples were rotated at 20000 Hz. The spectra were recorded at room temperature (296 K), and aqueous 85% H_3PO_4 was used as the external standard.

The reaction products were analyzed using a Hewlett–Packard HP 6890 gas chromatograph equipped with a 25-m Lipodex E or 50-m Chiraldex Gamma Cyclodextrin capillary column.

Table 1
Elemental analysis for parent and loaded materials[a]

Sample	Rh (mmol/g)	Al (mmol/g)	Si (mmol/g)	Si:Al
RhDuphos/Al-SBA-15	0.037	0.44	12.92	29.30
RhChiraphos/Al-SBA-15	0.019	0.45	12.85	28.55
RhProphos/Al-SBA-15	0.020	0.43	12.94	30.09
RhDiop/Al-SBA-15	0.035	0.44	12.91	29.34

[a] Theoretical rhodium content was 0.15 mmol/g.

3. Results and discussion

The X-ray powder diffraction of the siliceous SBA-15 showed the hexagonal structure characteristic for this material. It showed a well-resolved pattern with a prominent peak at 0.8° and two peaks at 1.4° and 1.6° 2θ, which match well with the pattern reported for SBA-15. This confirmed the successful synthesis of SBA-15 silica. The XRD peaks can be indexed to a hexagonal lattice with a $d(100)$ spacing of 110 Å, corresponding to a large unit cell parameter, $a_0 = 127$ Å ($a_0 = 2d(100)/\sqrt{3}$). The intensity of the reflection essentially did not change after the alumination or upon loading of the carrier with the organometallic complex.

Elementary analysis results for Rh, Si, and Al are presented in Table 1. The color transfer, during the immobilization in dichloromethane, from a orange solution to the white solid demonstrated a high degree of immobilization (Table 1, Rh content after immobilization in CH_2Cl_2), but upon extraction with methanol, which in contrast to the nonpolar dichloromethane adsorbs strongly on the Al-SBA-15 surface, the adsorbed complex desorbs from the silanol groups because of a competitive reaction with the polar alcohol.

A special case is the trial of immobilization of rhodium diphosphine complexes on an all-silica SBA-15 material (Table 2). After the first immobilization step in dichloromethane, the solid material had an orange color, and a Rh content of 0.07 mmol/g was found. After the extraction with methanol, the entire amount of organometallic complex was washed off, and the final material again had the original white color. No rhodium was detected in ICP-AS analyses of this sample. However, in the case of Al-SBA-15 the orange color obtained after the immobilization of the rhodium complexes in dichloromethane is clearly maintained, even after extraction in methanol.

N_2 sorption isotherms were measured for the pure carrier and for all immobilized complexes, respectively. Fig. 3 and Table 3 present a comparison of sorption isotherms and textural characteristics for pure and loaded samples. In all cases, these isotherms presented the characteristic form of mesoporous materials. It can easily be seen that the N_2 adsorbed/desorbed volume was higher in the case of pure carrier than in the case of immobilized complexes.

N_2 sorption isotherms of the supported catalysts showed a decrease in the surface area and in the mesopore volume of ca. 15% compared with the corresponding parent material. For example, the BET surface area was found to decrease from 467 m^2/g for the carrier material to 409 m^2/g for RhChiraphos/Al-SBA-15, with a corresponding decrease in mesopore volume from 0.92 to 0.83 cm^3/g. These results indicated that the complex was most likely deposited inside the pore system of Al-SBA-15.

Table 2
Rhodium content after immobilization in CH_2Cl_2 and extraction in MeOH

Sample	Rh content after	
	Immobilization in CH_2Cl_2 (mmol/g)	Extraction in MeOH (mmol/g)
RhDuphos/SBA-15	0.07	–
RhDuphos/Al-SBA-15	0.13	0.037
RhChiraphos/Al-SBA-15	0.11	0.019
RhProphos/Al-SBA-15	0.12	0.020
RhDiop/Al-SBA-15	0.12	0.035

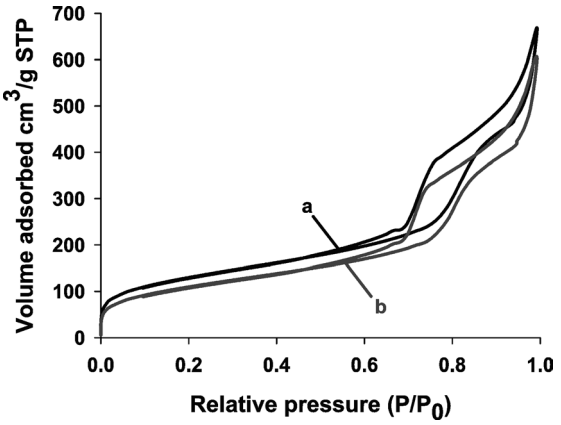

Fig. 3. N_2 adsorption isotherms of (a) Al-SBA-15 and (b) CODRhChiraphos immobilized on Al-SBA-15.

Table 3
Textural characteristics of parent Al-SBA-15 and loaded materials

Sample	Surface area (m^2/g)	Pore volume (cm^2/g)	Pore diameter (Å)
Al-SBA-15	467	0.92	94
RhDuphos/Al-SBA-15	397	0.78	89
RhChiraphos/Al-SBA-15	409	0.83	87
RhProphos/Al-SBA-15	412	0.83	88
RhDiop/Al-SBA-15	401	0.82	87

The infrared spectra of the loaded materials revealed the presence of bands attributed to the characteristic organic structure of the diphosphine complexes (Fig. 4). Although these bands are weak and not characteristic enough to resolve a structure, several typical bands could be distinguished, such as the =C–H band centered at 2962 and 2857 cm^{-1}. Furthermore, a medium-strength band at 1460 cm^{-1} was found, which could be assigned to the CH_2 bending vibration or P–C–H group. The weak band centered at 1440 cm^{-1} was assigned to the phosphorous-phenyl group. In accordance with the materials structure, the OH group stretching band centered at 3740 cm^{-1} is characteristic for terminal silanol groups. By comparison with the

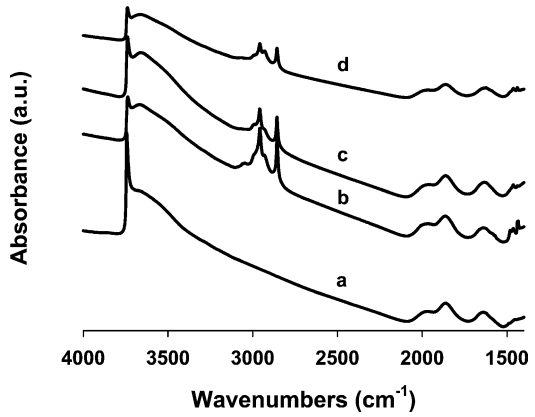

Fig. 4. IR spectra of (a) Al-SBA-15, (b) RhChiraphos/Al-SBA-15, and (c) RhDuphos/Al-SBA-15.

pure carrier, after the immobilization of rhodium diphosphine complexes, the intensity of this band decreased.

The acidity of the samples was characterized by FTIR spectroscopy investigation of adsorbed pyridine as a probe molecule. The spectra of adsorbed pyridine (Py) obtained after degassing at 200 °C are presented in Fig. 5. Pure all-silica materials have an electrically neutral framework and consequently showed no Lewis or Brønsted acidity. After the incorporation of aluminum, the FTIR spectra of adsorbed Py showed that both Lewis and Brønsted acid sites were created. The Al-SBA-15 prepared by postsynthesis alumination exhibited several peaks due to strong Lewis-bound pyridine (1623 and 1456 cm^{-1}), weak Lewis-bound pyridine (1577 cm^{-1}), and pyridinium ion on Brønsted acid sites (1546 and 1641 cm^{-1}), whereas all-silica SBA-15 showed only small peaks due to hydrogen-bonded pyridine (1446 and 1596 cm^{-1}). Moreover, after the immobilization of the organometallic complex a slight decrease in the Brønsted and Lewis acidity was observed. This decrease is due to guest/host interaction between the organometallic complex and the solid framework.

Temperature desorption of ammonia was used to characterize the acidity of all silica and aluminated SBA-15. The results are shown in Fig. 6. Comparison of the TPD curves of SBA-15 with that of Al-SBA-15 showed a dramatic increase of the acid strength and amount after alumination. The peaks with maxima at about 300 °C, found for both samples, were due to weakly bound ammonia (physisorbed ammonia, ammonia adsorbed on weak acid sites). The high-temperature peaks centered at 480 °C, which were much better defined in the case of Al-SBA-15, could be ascribed to ammonia desorbed from strong acid sites. These experiments clearly showed that acid sites were formed after alumination on the surface of the solid.

Quantitative loading of the organometallic complex was demonstrated with thermal gravimetric analysis. For all immobilized complexes, thermogravimetric and differential scanning calorimetric measurements showed a thermal stability up to 200 °C. In all cases, oxidation of the organic structure took place in two steps, corresponding to about

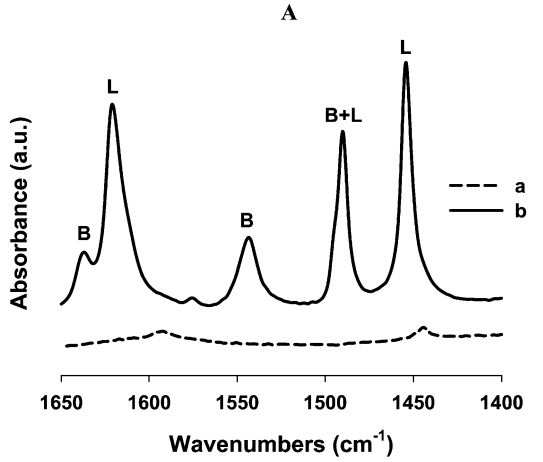

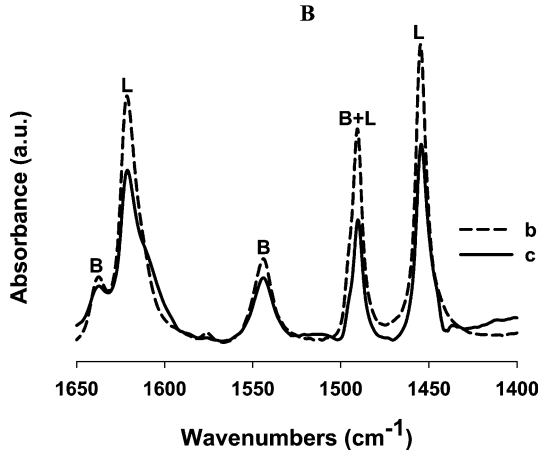

Fig. 5. IR spectra of adsorbed pyridine on (a) SBA-15, (b) Al-SBA-15, and (c) RhChiraphos/Al-SBA-15.

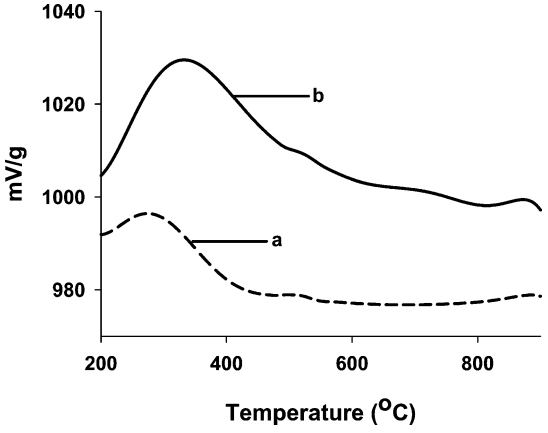

Fig. 6. Temperature-programmed desorption of ammonia of (a) SBA-15 and (b) Al-SBA-15.

250 or 400 °C, respectively (Fig. 7). The loss of ca. 3 wt% caused by burning of the complex was consistent with the content determined by chemical analysis. The oxidation of the pure carrier showed no characteristic peak.

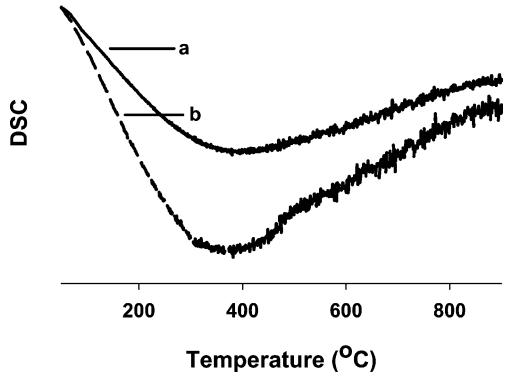

Fig. 7. DSC spectra of (a) Al-SBA-15 and (b) RhChiraphos/Al-SBA-15.

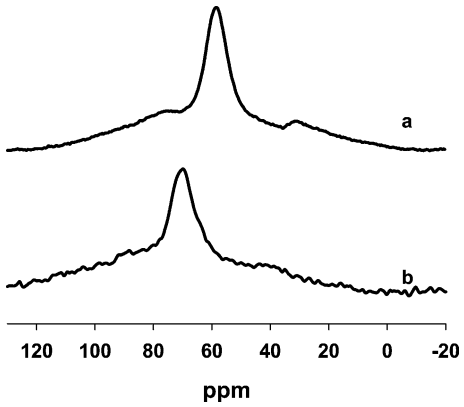

Fig. 8. ^{31}P MAS NMR of (a) homogeneous CODRhChiraphos and (b) CODRhChiraphos immobilized on Al-SBA-15.

To elucidate the chemical structure of the immobilized rhodium diphosphine complexes, MAS-NMR of the pure Al-SBA-15 carrier, the homogeneous complexes, and the immobilized complexes was recorded. Because of the low content of immobilized complex, the ^{13}C and ^{1}H resonance signals were too weak for quantitative interpretation. The pure carrier and immobilized complexes showed spectra for the ^{27}Al and ^{29}Si nuclei that were not significantly different. Therefore, the interpretation of a chemical shift is risky.

^{31}P MAS NMR spectra of the solid homogeneous CODRhChiraphos complex and the same complex immobilized on Al-SBA-15 are depicted in Fig. 8. The homogeneous complex gave a strong signal at 59 ppm and two weaker ones at 30 and 75 ppm due to trace amounts of oxidic impurities. The MAS NMR spectrum of the immobilized CODRhChiraphos complex showed only a single signal at 71 ppm. The absence of signals of the free phosphine ligand was an indication that the phosphine ligand was completely coordinated to the rhodium. The immobilization of this rhodium Chiraphos complex led to a shift of the ^{31}P signal of 12 ppm to a lower magnetic field compared with the homogeneous complex as the result of the interaction of the guest complex with the surface of the Al-SBA-15 host, more specifically the interaction with a Lewis acidic center on the surface, which withdraws electrons from the rhodium metal or the phosphine ligand and thus lowers the electron density.

Fig. 9. Substrates used in enantioselective hydrogenation.

The rhodium complexes used consisted of a chiral diphosphine and a cyclooctadiene ligand. There could be several forces involved in the bonding of the complex to Al-SBA-15. For example, an electrostatic interaction of the cationic complexes with the anionic framework of the Al-SBA-15 structure could occur. A similar mechanism was reported for the immobilization of manganese complexes on Al-MCM-41 [28], as well as for immobilized rhodium complexes on Al-MCM-41 [18]. Furthermore, direct bridging of the rhodium to surface oxygen of the mesoporous walls has also been observed and could occur after cleavage of the diene complex during the hydrogenation reaction [29]. However, no evolution of cyclooctadiene during the immobilization reaction could be observed, and FT-IR spectra of the filtrate obtained after impregnation did not contain bands attributable to free cyclooctadiene.

3.1. Catalytic properties

Several diphosphine ligands have been applied, and the corresponding complexes have been tested for immobilization. The activities of the different free and immobilized catalysts in several enantioselective hydrogenation reactions were investigated (Fig. 9). In a blank reaction using the parent material, no reaction took place, whereas over Rh supported on Al-SBA-15 no enantiomeric excess was observed, although conversions up to 99% were found. Moreover, for all hydrogenation experiments the chemical selectivity was 100%. No side products were observed.

The hydrogenation of dimethyl itaconate and methyl α-acetamidoacrylate over free and immobilized rhodium complexes was carried out at a substrate/rhodium ratio of 1000. For the hydrogenation of dimethyl itaconate over the free complexes, between 90 and 94% e.e. was observed at quantitative conversion. The S,S-Me-Duphos ligand reached the best results, with 94% e.e. in homogeneous media and 89% enantioselectivity at $>$ 99% conversion for the immobilized complex (TOF $= 44\ h^{-1}$). The corresponding supported catalysts with S,S-Chiraphos and R-Prophos showed enantioselectivities of 72% e.e. and 79% e.e. at 96 or 89% conversion, respectively. For the immobilized R,R-Diop complex, 68% e.e. at 95% conversion was found. In the case of immobilized RhDuphos complex the determined turnover number was 1000. However, with standard procedures the catalyst could be recycled four times without any loss of activity or selectivity; that is, the TON was 4000.

For the hydrogenation of methyl α-acetamidoacrylate over the free complexes, enantiomeric excesses of 86 to 94% and quantitative conversions were obtained. Again, the

S,S-Me-Duphos ligand showed the best results. The homogeneous complex showed an enantioselectivity of 94%, and over the corresponding heterogeneous catalyst 93% e.e. at $> 99\%$ conversion was found (TOF $= 43\ h^{-1}$). Furthermore, the immobilized complex of S,S-Chiraphos and R-Prophos showed good enantioselectivities of 77% at 92% conversion, or 78% e.e. at 94% conversion, respectively. With the immobilized complex of R,R-Diop, 62% e.e. at a corresponding conversion of 95% was found. Again, the catalysts were recovered and reused without further treatment. The supported RhDuphos catalyst was recycled 10 times. The conversion and the enantioselectivity of the catalyst remained at high levels for more than four runs. After 8 to 10 consecutive runs, a decrease in catalytic performance was observed. This phenomenon is consistent with the formation of lumps in the catalyst. Organic deposits like polymerization products of the substrate lead to such deactivation. However, they could not be identified by spectroscopic analysis.

To prove that the reaction was catalyzed heterogeneously and to exclude the possibility of leaching and homogeneous catalysis, the reaction mixture was separated from the catalyst before complete conversion occurred (hot filtration test) [30]. For hydrogenation of dimethyl itaconate, removal of the RhDuphos immobilized on Al-SBA-15 effectively stopped the reaction after 6 h. After 24 h the conversion of the filtered sample remained at 42%, whereas the original batch with catalyst was converted completely. This proved that no homogeneous catalysis took place. ICP AES analysis of the filtered reaction solution showed traces of rhodium, phosphorus, silicon, and aluminum, in relative amounts corresponding to the composition of the heterogeneous catalyst, indicating that this loss occurred by attrition of the Al-SBA-15 rather than by leaching of the complex, because the mixture was vigorously stirred. Similar results were obtained for the hydrogenation of methyl α-acetamidoacrylate with immobilized RhChiraphos.

In our former work, Al-MCM-41 and Al-MCM-48 were used as support materials for the rhodium diphosphine complexes [18,31]. For the hydrogenation of dimethyl itaconate with RhDuphos immobilized on Al-MCM-41, an enantiomeric excess of 92% at a corresponding TOF of 166 h^{-1} was obtained, whereas the same complex immobilized on Al-MCM-48 gave 98% e.e. at a corresponding TOF of 234 h^{-1}. When methyl α-acetamidoacrylate was hydrogenated over RhDuphos immobilized on Al-MCM-41, an enantiomeric excess of 97% at a corresponding TOF of 83 h^{-1} was observed, whereas the same complex immobilized on Al-MCM-48 gave 97% e.e. at a corresponding TOF of 120 h^{-1}. Considering these results, it was obvious that the activity of the immobilized rhodium complexes could be increased by a faster diffusion of the substrate and products inside the pore system. Unfortunately, over SBA-15-type materials, which should show smaller diffusion limitation because of their large pore system, the activity of the immobilized rhodium diphosphine complexes was surprisingly lower than that of M41S-type materials as supports. The M41S solids were synthesized as aluminum-containing materials, whereas the SBA-15 material used here was aluminated by postsynthesis treatment. The difference in synthesis/postsynthesis alumination might affect the host-guest interaction and influence the activity of the immobilized complexes. It might also be possible that stronger constraints in the M41S materials with a smaller pore size compared with the SBA-15 caused such an effect. Right now, we have no clear understanding of these unexpected results.

4. Conclusions

New heterogeneous chiral catalysts were prepared from chiral rhodium diphosphine complexes and Al-SBA-15. The complexes were bonded to the carrier by the interaction of the cationic rhodium of the organometallic complex with the anionic host framework, as well as between Al Lewis acid sites and P Lewis basic sites. This method is effective and simpler than covalent bonding of guest molecules.

The immobilized catalysts showed high activities and excellent chemo- and enantioselectivities, achieving up to 93% e.e., at $> 99\%$ conversion and 99% selectivity. The results indicated that the stereochemistry of the product was mainly dictated by the chirality of the diphosphine ligands. The activity of the immobilized complexes on Al-SBA-15 was lower than that obtained with M41S-type materials as supports.

The recyclability of rhodium diphosphine complexes immobilized on Al-SBA-15 was demonstrated with standard procedures. The catalysts could be reused at least four times without any activity loss, with a TON larger than 4000.

The high activities observed with these supported organometallic complexes, plus the fact that the high activity is maintained upon reuse of the catalysts, indicated that these are truly heterogeneous counterparts of homogeneous transition-metal complexes.

Acknowledgment

The authors are very grateful for the financial support from the Sonderforschungsbereich SFB 380 of the Deutsche Forschungsgemeinschaft (DFG).

References

[1] E.N. Jacobsen, A. Pfltaz, H. Yamamoto (Eds.), Comprehensive Asymmetric Catalysis, vols. I–III, Springer, Berlin, 1999.
[2] I. Ojima (Ed.), Catalytic Asymmetric Synthesis, second ed., Wiley–VCH, New York, 2000.
[3] H.U. Blaser, F. Spindler, M. Studer, Appl. Catal. A 221 (2001) 119.
[4] W.S. Knowless, Angew. Chem. Int. Ed. 41 (2002) 1998.
[5] R. Noyori, Angew. Chem. Int. Ed. 41 (2002) 2008.
[6] K.B. Sharpless, Angew. Chem. Int. Ed. 41 (2002) 2024.
[7] H.U. Blaser, Chem. Commun. (2003) 293.

[8] T. Ohkuma, H. Takeno, Y. Honda, R. Noyori, Adv. Synth. Catal. 343 (2001) 369.
[9] B.F.G. Johnson, S.A. Raynor, D.S. Shephard, T. Mashmeyer, J.M. Thomas, G. Sankar, S. Brolmley, R. Oldroyd, L. Gladden, M.D. Mantle, Chem. Commun. (1999) 139.
[10] A. Mandaloni, D. Pini, S. Orlandi, F. Manzini, P. Salvadori, Tetrahedron: Asymmetry 9 (1998) 1479.
[11] A. Wolfson, S. Janssens, I. Vankelcom, S. Geresh, M. Gottlieb, M. Herkowitz, Chem. Commun. (2002) 388.
[12] J. Jamis, J.R. Anderson, R.S. Dickson, E.M. Campi, W.R. Jackson, J. Organomet. Chem. 627 (2001) 37.
[13] S.B. Ogunwami, T. Bein, Chem. Commun. (1997) 901.
[14] M.J. Sabatier, A. Corma, A. Domenech, V. Fornes, H. Garcia, Chem. Commun. (1997) 1285.
[15] C. Schuster, E. Mollmann, A. Tompos, W.F. Hölderich, Catal. Lett. 74 (2001) 69.
[16] C. Bianchini, P. Barbaro, V. Dal Santo, R. Gobetto, A. Meli, W. Oberhauser, R. Psaro, F. Vizza, Adv. Synth. Catal. 343 (2001) 41.
[17] R. Augustine, S. Tanielyan, S. Anderson, H. Yang, Chem. Commun. (1999) 1257.
[18] H. Wagner, H. Hausmann, W.F. Hölderich, J. Catal. 203 (2001) 150.
[19] C.E. Song, S.G. Lee, Chem. Rev. 19 (2002) 3495.
[20] C. Bianchini, P. Barbaro, Top. Catal. 19 (2002) 17.
[21] P. McMorn, G.J. Hutchings, Chem. Soc. Rev. 33 (2004) 108.
[22] D.E. De Vos, I.F.J. Vankelecom, P.A. Jacobs (Eds.), Chiral Catalyst Immobilization and Recycling, Wiley–VCH, Weinheim, 2000.
[23] D. Zhao, J. Feng, Q. Huo, N. Melosh, G.H. Frederickson, B.F. Chmelka, G.D. Stucky, Science 279 (1998) 548.
[24] D. Zhao, Q. Huo, J. Feng, B.F. Chmelka, G.D. Stucky, J. Am. Chem. Soc. 120 (1998) 6024.
[25] J. Fan, C. Yu, L. Wang, B. Tu, D. Zhao, Y. Sakamoto, O. Terasaki, J. Am. Chem. Soc. 123 (2001) 12113.
[26] Z. Luan, M. Hartmann, D. Zhao, W. Zhou, L. Kevan, Chem. Mater. 11 (1999) 1621.
[27] M. Cheng, Z. Wang, K. Sakurai, F. Kumata, T. Saito, T. Komatsu, T. Yashima, Chem Lett. (1999) 131.
[28] S.S. Kim, W. Zhang, T.J. Pinnavaia, Catal. Lett. 43 (1997) 149.
[29] A. Janssen, J.P.M. Niederer, W.F. Hölderich, Catal. Lett. 48 (1997) 165.
[30] H.E.B. Lempers, R.A. Sheldon, J. Catal. 175 (1998) 62.
[31] A. Crosman, W.F. Hoelderich, in: Proceedings: 14th International Zeolite Conference, Cape Town, South-Africa, 25–30 April, 2004.